Hindawi
Modelling and Simulation in Engineering
Volume 2023, Article ID 6069078, 15 pages
https://doi.org/10.1155/2023/6069078

Research Article

Investigate the Relationship between the Vehicle Roll Angle and Other Factors When Steering

Duc Ngoc Nguyen and Tuan Anh Nguyen

Automotive Engineering Department, Thuyloi University, Hanoi, Vietnam

Correspondence should be addressed to Duc Ngoc Nguyen; ndn@tlu.edu.vn

Received 20 October 2022; Revised 15 January 2023; Accepted 18 January 2023; Published 28 January 2023

Academic Editor: Angelos Markopoulos

Rollover is a dangerous phenomenon. It is closely related to the vehicle roll angle. The greater the roll angle, the greater the risk of rollover. The vehicle roll angle when steering depends on many factors, such as the size of the vehicle, speed of movement, steering angle, etc. In this paper, the author has simulated the oscillation of a car when steering using MATLAB® software with three specific cases. The purpose of the study is to evaluate the dependence of the roll angle on other factors. Each case handles two scenarios: vehicle speed change (fixed height) and vehicle height change (fixed speed). The model of a complex dynamic, a combination of many nonlinear components, is used to simulate vehicle oscillations. According to the study's results, the roll angle will increase if the speed or the distance from the center of gravity (CG) to roll axis (RA) increases, respectively. Once the roll angle's value rises, the roll index also increases, which causes the dynamic force at the wheel to decrease. If the vertical force at the wheel approaches zero, a rollover may occur. The rollover phenomenon occurred in the second case, corresponding to speeds $v = 80$ (km/h) and $v = 85$ (km/h). The peak values of the roll angle are 7.77° and 7.63°, respectively. This result helps to identify the factors affecting the rollover phenomenon more clearly.

1. Introduction

Since more than 130 years ago, the automotive sector has seen significant growth. Today's automobiles are far more extensive and faster compared to the past. Therefore, the stability and safety of the vehicle are crucial concerns that require complete attention. Several phenomena may be used to illustrate the instability of a moving car on the road, with vehicle rollover being the most hazardous. Rollover incidents can have severe repercussions for individuals and items [1].

The phenomenon of rolling over happens when the wheels are completely pushed off the road, i.e., when the dynamic force at the wheels approaches zero [2–4]. Regarding the problem of rolling, the wheel cannot return to its previous position after being lifted off the road. Once the vertical force on the wheel is zero, the roll angle may reach its highest limit [5]. Rollovers typically occur when a vehicle steer to avoid an obstruction or enters a roundabout [6]. Then, centrifugal force may appear. This force will create a moment that tilts the vehicle body [7]. There are four typical reasons for rollovers. Initially, external elements such as wind force might influence a vehicle's performance in inclement weather [8]. Nevertheless, the value of the lateral wind force is typically insignificant. A few instances of heavy truck rollover are due to the lateral wind force. The second factor contributing to this occurrence is road conditions [9]. Besides, the size of the vehicle also affects this problem. The roll moment of a car will grow according to the track-width and height, and this was emphasized by Nguyen et al. [10]. Because adjusting the size of the vehicle may impact its performance, it is not simple to do so. The third factor relating to this phenomenon is the vehicle's speed. This is considered the primary source of the occurrence of rollover. If the velocity is more, the centrifugal force will grow according to the velocity's square. Consequently, the risk of a rollover will increase. Lastly, the value of the steering acceleration and steering angle significantly impact the

issue of vehicle instability. If these values rise, the rollover limitation will reduce fast, making the vehicle more susceptible to rolling.

Li and Bei developed the notion of a static roll index in reference [11]. This index is only dependent on the size of the vehicle, according to Xin et al. [12]. However, this indicator is not significant. The dynamic roll index thereby substitutes the static roll index, which describes the rollover phenomenon more clearly, commonly known as load transfer ratio (LTR) [13]. This index is a result of the differential in dynamic force between the wheels, according to Jin et al. [14]. As soon as the value of this indicator exceeds 1, the car rolls over. This indicator is utilized in a large number of rollover research [15, 16].

In the study of roll dynamics, several dynamical models are routinely employed. Zhang et al. merged a 1/2 model and a single-track dynamics model [17]; this is a typical design. However, it is relatively straightforward, and the accuracy is typically low. This model handles the tire as a linear deformation [18]. The vehicle's motion should be evaluated completely using a spatial dynamics model. This model accounts for the impact of all wheels [19]. It may be utilized for both commercial and specialized vehicles [20]. Nonlinear double-track dynamics must be included in the model of spatial dynamics. In reference [21], Nguyen performed this combo. However, constructing this model is quite difficult. Today, multiple methods have been implemented to improve the vehicle's stability at high speeds. According to Nguyen, the stabilizer bar can decrease the body roll angle during steering [22]. Moreover, the adaptive suspension system enhances the vehicle's stability [23–26]. In addition, redistributing power to the driving wheels helps lower the incidence of rollover [27]. If the rollover limits are predefined, the phenomena of rollover may be accurately predicted. Several methods are used to determine the roll limit, such as predicting the vehicle's roll angle [28–30], the roll index [3, 4], etc. In general, they are quite complex.

Additionally, there are many solutions used to avoid rollovers. In reference [31], Bencatel et al. propose the application of the reference governors (RG) to control the car steering system. In reference [32], Edlund et al. introduce the use of the rollover protection systems (ROPS) anti-roll system for quad bikes. The sharing of the active steering (AS) and active anti-roll bar (AARB) to reduce the rollover phenomenon has been shown in reference [33] by Liu et al. Nguyen et al. also show in reference [34] how to use an active stabilizer bar to reduce the roll angle of the vehicle body. In addition, many other control algorithms that help limit the rollover phenomenon have also been introduced by many authors [35, 36]. In addition, many studies examining the dependence of rollover on other factors have also been published in the past few years. For instance, in reference [37], Alrejjal et al. indicate variables related to external factors, such as weather, roadways, etc. In reference [38], Hassan et al. state the influence of tires on lateral stability and rollover when steering. Besides, the vehicle's mass also dramatically influences the vehicle's rolling stability, according to Alrejjal and Ksaibati [39]. However, studies on the influence of vehicle speed and height on rollover are rarely done, although this is a significant issue. Therefore, it is necessary to investigate the dependence between height, speed, and the rollover phenomenon.

As mentioned above, the rollover phenomenon is closely related to the vehicle roll angle. If the roll angle is too large, this phenomenon may occur. The roll angle depends on many factors, such as the size of the vehicle and the use of the vehicle by the driver. Therefore, it is necessary to determine the relationship between them. This paper focuses on surveying and evaluating the relationship between the vehicle roll angle and the vehicle's height, travel speed, and steering angle. A complex dynamic model is used to simulate car oscillations under specific circumstances. This is completely new and practical content. The main content of this paper consists of four parts, including an introduction section, materials section, results section, and conclusions section. The specific contents will be presented in turn in this order.

2. Materials

To simulate car oscillations, a complex dynamic model needs to be built. This model includes smaller components, such as the spatial oscillation model, the tire model, and the motion model. These models are referenced in [3, 4, 21].

The spatial oscillation model is described in Figure 1. Equations (1) to (11) are used to describe this model.

Total forces acting on the sprung mass:

$$F_{ims} = \sum_{i,j=1}^{2} \left(F_{Kij} + F_{Cij}\right). \tag{1}$$

Total moments acting on the vehicle body (roll):

$$M_{\phi} = \sum_{i,j=1}^{2} \left[(-1)^{j-1}\left(F_{Kij} + F_{Cij}\right)t_{wi}\right]$$

$$+ \left\{ g sin\phi + \left[\dot{v}_y + \left(\dot{\beta} + \dot{\psi}\right)v_x\right] \cos\phi \right\} m_s h_{\phi}. \tag{2}$$

Total moments acting on the vehicle body (pitch):

$$M_{\theta} = \sum_{i,j=1}^{2} (-1)^{i-1}\left(F_{Kij} + F_{Cij}\right)a_i. \tag{3}$$

Total forces acting on the unsprung masses:

$$F_{imuij} = F_{KTij} - F_{Kij} - F_{Cij}i, \quad j = \overline{1,2}. \tag{4}$$

Where:
Force of inertia (sprung mass), F_{ims}:

$$F_{ims} = m_s \ddot{z}_s i, \quad j = \overline{1,2}. \tag{5}$$

Force of inertia (unsprung mass), F_{imuij}:

$$F_{imuij} = m_{uij} \ddot{z}_{uij} i, \quad j = \overline{1,2}. \tag{6}$$

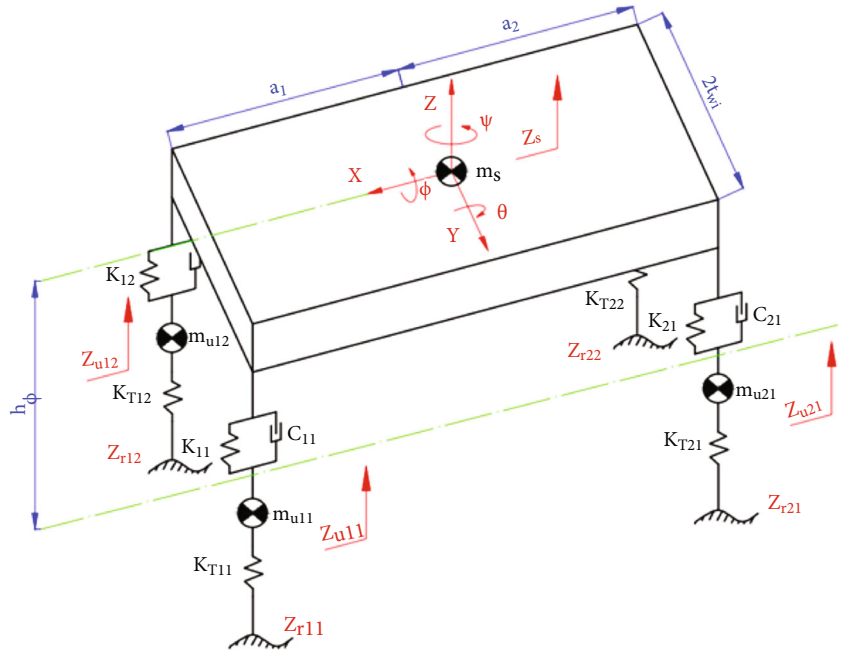

Figure 1: A model of the oscillation.

Force of spring, F_{Kij}:

$$F_{Kij} = K_{ij}\left[z_s - z_{uij} + (-1)^{j+1}t_{wi}\phi + (-1)^{i+1}a_i\theta\right] i, j = \overline{1,2}. \quad (7)$$

Force of damper, F_{Cij}:

$$F_{Cij} = C_{ij}\left[\dot{z}_s - \dot{z}_{uij} + (-1)^{j+1}t_{wi}\dot{\phi} + (-1)^{i+1}a_i\dot{\theta}\right] i, j = \overline{1,2}. \quad (8)$$

Force of tire, F_{KTij}:

$$F_{KTij} = K_{Tij}\left(z_{rij} - z_{uij}\right) i, j = \overline{1,2}. \quad (9)$$

Moment of inertia (roll), M_ϕ:

$$M_\phi = \left(J_\phi + m_s h_\phi^2\right)\ddot{\phi}. \quad (10)$$

Moment of inertia (pitch), M_θ:

$$M_\theta = \left(J_\theta + m_s h_\theta^2\right)\ddot{\theta}. \quad (11)$$

The components related to motion, such as lateral velocity v_y, longitudinal velocity v_x, and yaw angle ψ, are unknowns. They can be calculated through a motion model with three degrees of freedom (Figure 2).

Total forces acting on the vehicle (longitudinal):

$$F_{ix} = \sum_{i,j=1}^{2}\left(F_{xij}\cos\delta_{ij} - F_{yij}\sin\delta_{ij}\right) - F_1 + F_{cex}. \quad (12)$$

Total forces acting on the vehicle (lateral):

$$F_{iy} = \sum_{i,j=1}^{2}\left(F_{xij}\sin\delta_{ij} + F_{yij}\cos\delta_{ij}\right) - F_2 - F_{cey}. \quad (13)$$

Total moments acting on the vehicle (yaw):

$$M_\psi = \sum_{i,j=1}^{2}\left[(-1)^j\left(F_{xij}\cos\delta_{ij} - F_{yij}\sin\delta_{ij}\right)t_{wi}\right.$$

$$\left. + (-1)^{i+1}\left(F_{xij}\sin\delta_{ij} + F_{yij}\cos\delta_{ij}\right)a_i + F_i c_i - M_{zij}\right]. \quad (14)$$

Where:
Force of inertia (longitudinal):

$$F_{ix} = \left(m_s + \sum_{i,j=1}^{2} m_{ij}\right)\dot{v}_x. \quad (15)$$

Force of inertia (lateral):

$$F_{iy} = \left(m_s + \sum_{i,j=1}^{2} m_{ij}\right)\dot{v}_y. \quad (16)$$

Centrifugal force (longitudinal):

$$F_{cex} = \left(m_s + \sum_{i,j=1}^{2} m_{ij}\right)\left(\dot{\beta} + \dot{\psi}\right)v_y. \quad (17)$$

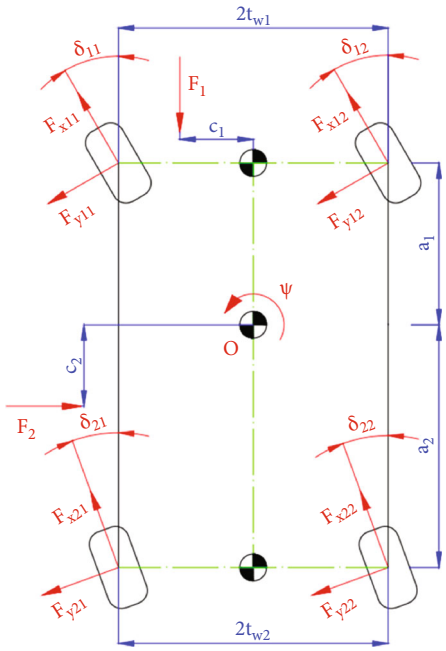

Figure 2: A model of the motion.

Centrifugal force (lateral):

$$F_{cey} = \left(m_s + \sum_{i,j=1}^{2} m_{ij}\right)\left(\dot{\beta} + \dot{\psi}\right)v_x. \tag{18}$$

Moment of inertia (yaw):

$$M_\psi = J_\psi \ddot{\psi}. \tag{19}$$

Heading angle:

$$\beta = \arctan\frac{v_y}{v_x}. \tag{20}$$

The longitudinal force, lateral force, and moment at the wheel can be determined by the tire model. Tire modelling can be simple or complex, depending on the intended use of the studies. In this work, the author proposes using the Pacejka tire model to determine the above unknowns.

Longitudinal force:

$$F_x = D_x \sin\left[C_x \text{artan}(B_x\kappa_x)\right]. \tag{21}$$

Where:

$$\kappa_x = (1 - E_x)\lambda + \frac{E_x}{B_x}\arctan\left(B_x\lambda\right). \tag{22}$$

$$C_x = 1.65. \tag{23}$$

$$D_x = a_1 F_z{}^2 + a_2 F_z. \tag{24}$$

$$BCD_x = \frac{a_3 F_z{}^2 + a_4 F_z}{e^{a_5 F_z}}, \tag{25}$$

$$B_x = \frac{BCD_x}{C_x D_x}, \tag{26}$$

$$E_x = a_6 F_z{}^2 + a_7 F_z + a_8. \tag{27}$$

Lateral force:

$$F_y = D_y \sin\left[C_y \text{ar tan}\left(B_y\kappa_y\right)\right] + S_{vy}. \tag{28}$$

Where:

$$\kappa_y = \left(1 - E_y\right)\left(\alpha + S_{hy}\right) + \frac{E_y}{B_y}\arctan\left[B_y\left(\alpha + S_{hy}\right)\right]. \tag{29}$$

$$C_y = 1.30. \tag{30}$$

$$D_y = a_1 F_z{}^2 + a_2 F_z, \tag{31}$$

$$BCD_y = a_3 \sin\left[a_4 \text{ar tan}\left(a_5 F_z\right)\right], \tag{32}$$

$$B_y = \frac{BCD_y}{C_y D_y}, \tag{33}$$

$$E_y = a_6 F_z{}^2 + a_7 F_z + a_8, \tag{34}$$

$$S_{hy} = a_9\gamma, \tag{35}$$

$$S_{vy} = \left(a_{10} F_z{}^2 + a_{11} F_z\right)\gamma. \tag{36}$$

Aligning moment:

$$M_z = D_z \sin\left[C_z \text{ar tan}\left(B_z\kappa_z\right)\right] + S_{vz}. \tag{37}$$

Where:

$$\kappa_z = (1 - E_z)(\alpha + S_{hz}) + \frac{E_z}{B_z}\arctan\left[B_z(\alpha + S_{hz})\right], \tag{38}$$

$$C_z = 2.40, \tag{39}$$

$$D_z = a_1 F_z{}^2 + a_2 F_z, \tag{40}$$

$$BCD_z = \frac{a_3 F_z{}^2 + a_4 F_z}{e^{a_5 F_z}}, \tag{41}$$

$$B_z = \frac{BCD_z}{C_z D_z}, \tag{42}$$

$$E_z = a_6 F_z{}^2 + a_7 F_z + a_8, \tag{43}$$

$$S_{hz} = a_9\gamma, \tag{44}$$

$$S_{vz} = \left(a_{10} F_z{}^2 + a_{11} F_z\right)\gamma. \tag{45}$$

After the dynamic modelling process is completed, the simulation process will take place.

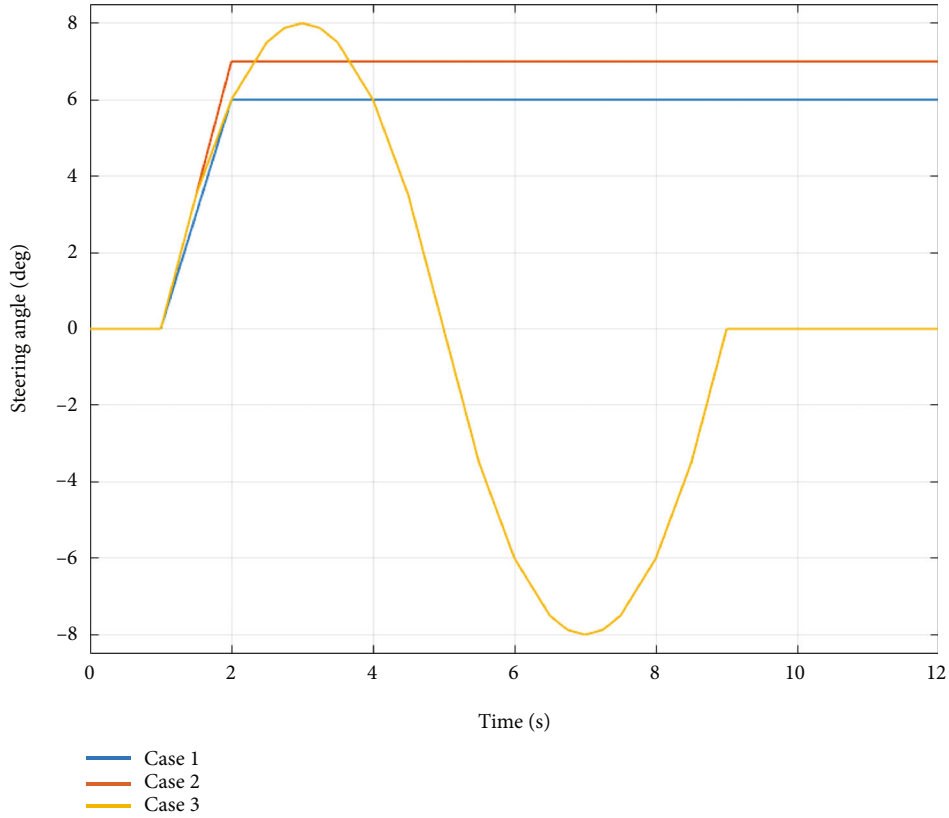

Figure 3: Steering angle.

3. Results

Numerical simulation is performed to evaluate the dependence of the roll angle on other factors. MATLAB® software is used for this purpose. Three cases correspond to the three steering angles used to simulate car oscillations (Figure 3). These three steering angles have differences in both magnitude and steering acceleration. Their values are not much different but can be enough to cause a rollover (for the second case and third case) when the vehicle travels at high speed. In each case, the vehicle speed and height will be varied to determine this relationship. The parameters that serve the simulation process are given in Table 1. These values are referenced in the CARSIM® application. CARSIM® software is a specialized application for simulating car oscillations. This software can be used independently or in conjunction with other software, such as MATLAB® [40], Python® [41], and LabVIEW® [42]. Many studies often refer to the specifications of cars using this software. Some parameters can be slightly adjusted to suit the actual conditions.

3.1. The First Case. In the first case, the steering angle is minor (Figure 3). The dependence of the roll angle on the velocity is shown in Figure 4. In this case, the distance from center of gravity (CG) to roll axis (RA) is constant, with $h = 550$ (mm). It is clear that the roll angle will increase if the vehicle speed increases. According to this result, the peak of the roll angle reached 4.84°, 5.37°, 5.90°, and 6.43°, respectively, corresponding to the speed range from 60 to 75 (km/h). When the speed increases up to $v = 80$ (km/h), the maximum value of the roll angle will continue to increase, reaching 6.94°. This number can go up to 7.47° once the velocity reaches the limit of the investigation process, $v = 85$ (km/h). After these values peak, they tend to decrease over time, even though the steering angle does not change. This happens because of elastic tire deformation, which is described by a complex nonlinear tire model. These values tend to converge in a specific domain. However, there is still a small difference between the values. The most significant decline is when the vehicle moves at top speed and vice versa.

When the vehicle body roll angle changes, the rollover index (RI) value also changes accordingly. The change in RI is depicted in Figure 5. The trend of the change in the values in Figure 5 is similar to the values in Figure 4. The peak of the values is still reached at time $t \approx 3.7$ (s). This is the time after the steering angle has reached its maximum at $t = 2$ (s). The maximum roll index obtained is 0.93, corresponding to a speed of $v = 85$ (km/h). If the velocity decreases, the value of RI also decreases accordingly. The values of RI obtained are 0.87, 0.80, 0.74, 0.67, and 0.60, respectively, corresponding to the speed range $v = \{80; 75; 70; 65; 60\}$ (km/h). After reaching the peak, their values will gradually decrease and converge in a certain domain.

If the vehicle's speed is fixed and the distance from CG to RA varies, the vehicle's roll angle also changes according to the value of the distance. Compared with the two graphs above, the changing trend of the values in Figure 6 is different. However, this difference is not so significant. According

Table 1: The simulation parameters.

No.	Symbol	Description	Value	Unit
1	K_{11}/K_{12}	Spring stiffness of the front axle	45,200	N/m
2	K_{21}/K_{22}	Spring stiffness of the rear axle	44,600	N/m
3	K_{T11}/K_{T12}	Spring tire of the front axle	178,000	N/m
4	K_{T21}/K_{T22}	Spring tire of the rear axle	178,000	N/m
5	C_{11}/C_{12}	Damper coefficient of the front axle	3300	Ns/m
6	C_{21}/C_{22}	Damper coefficient of the rear axle	3220	Ns/m
7	m_s	Sprung mass	1740	kg
8	m_{uij}	Unsprung mass	41	kg
9	t_{wi}	Half of the track width front/rear axle	805/815	mm
10	a_i	The distance between the center of gravity to the front or rear axle	1190/1360	mm
11	J_ϕ	Moment of inertia (longitudinal-axis)	720	kg/m^2
12	J_θ	Moment of inertia (lateral-axis)	2700	kg/m^2
13	J_ψ	Moment of inertia (vertical-axis)	2680	kg/m^2

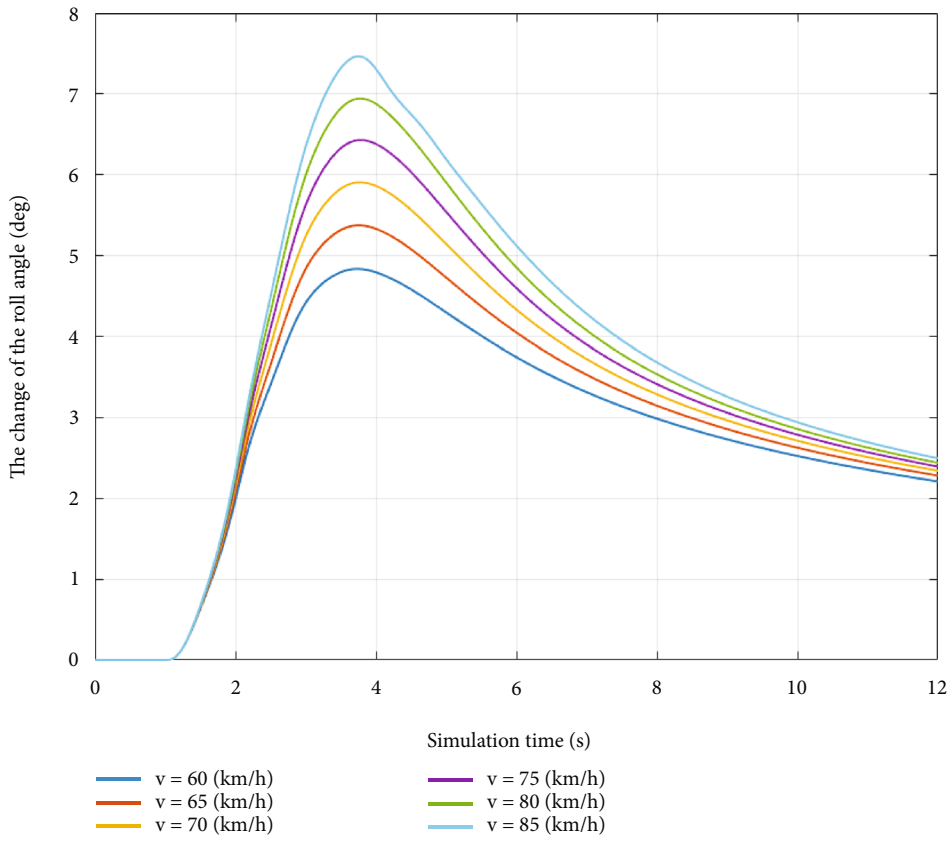

Figure 4: The change of the roll angle (the first case—velocity change).

to this finding, the roll angle will increase once the distance from CG to RA increases accordingly. Their peak values are still reached at $t \approx 3.7$ (s), then gradually decreasing over time. The difference between the values corresponding to the distances is not large and relatively even. The peak value of the roll angle corresponding to $h = 550$ (mm) is only 4.84°, while this value can reach 5.82° if the distance increases to $h = 650$ (mm).

Because the difference in roll angles for different distances is not too much, the change of RI, in this case, is not too significant (Figure 7). The changing trend of RI still follows the changing direction of the vehicle roll angle, which has been proved by the results obtained above. In this case, the difference between RI_{min} and RI_{max} is only about 0.14, and the gap between the values is quite even.

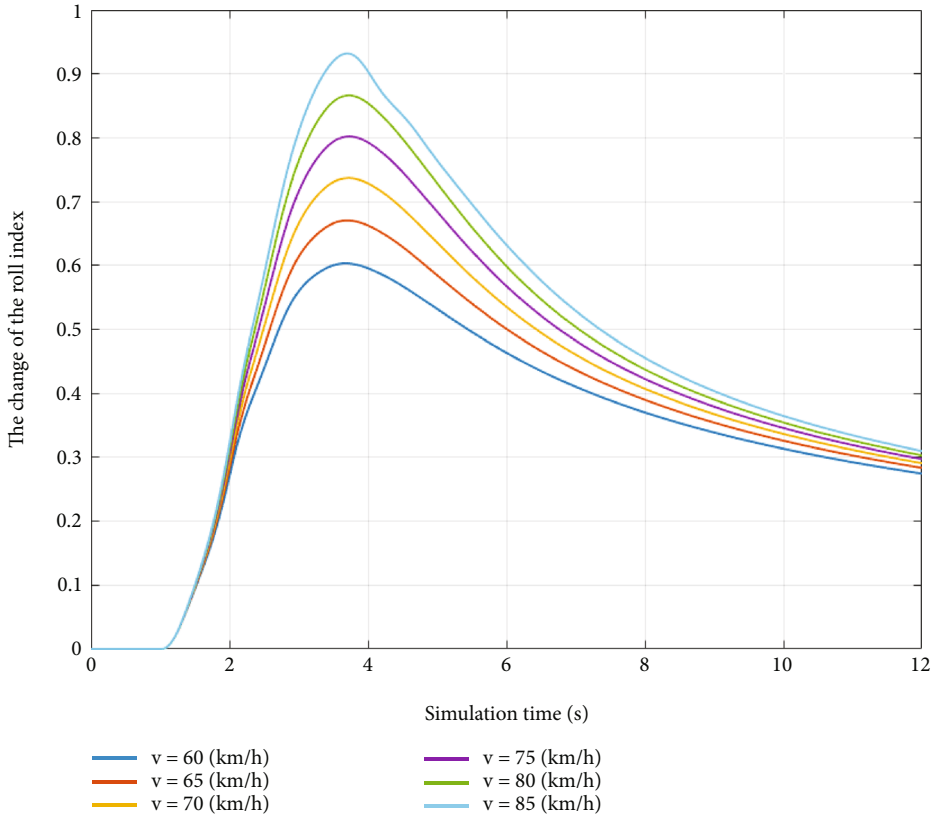

Figure 5: The change of the roll index (the first case—velocity change).

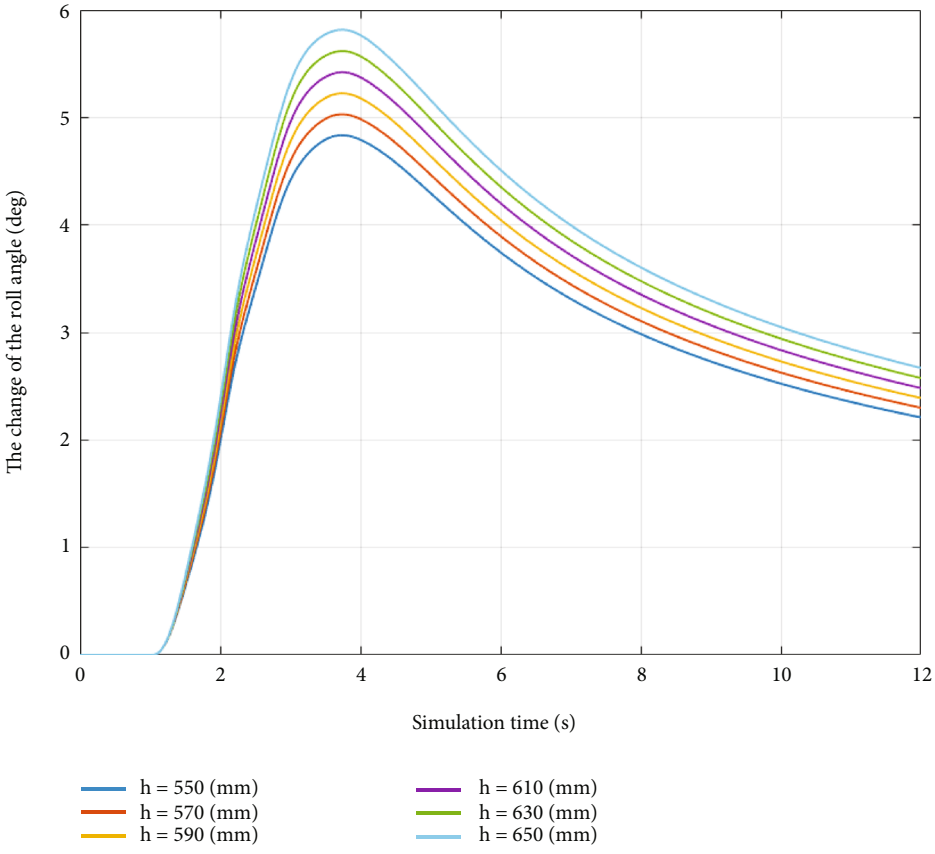

Figure 6: The change of the roll angle (the first case—distance change).

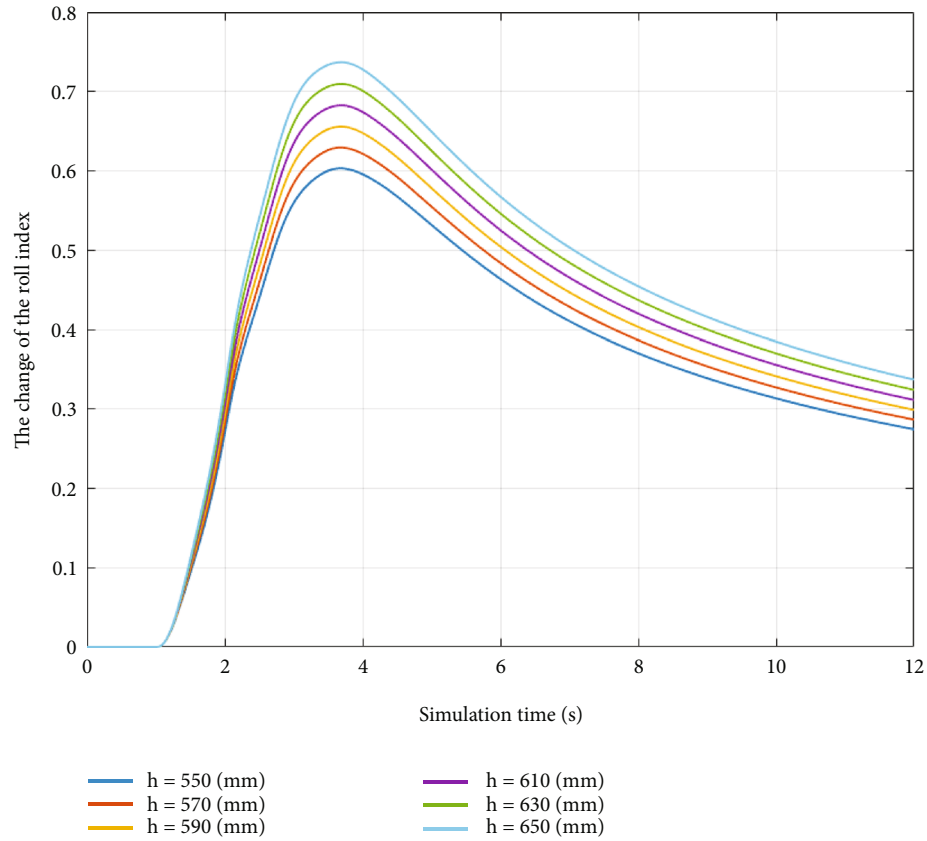

Figure 7: The change of the roll index (the first case—distance change).

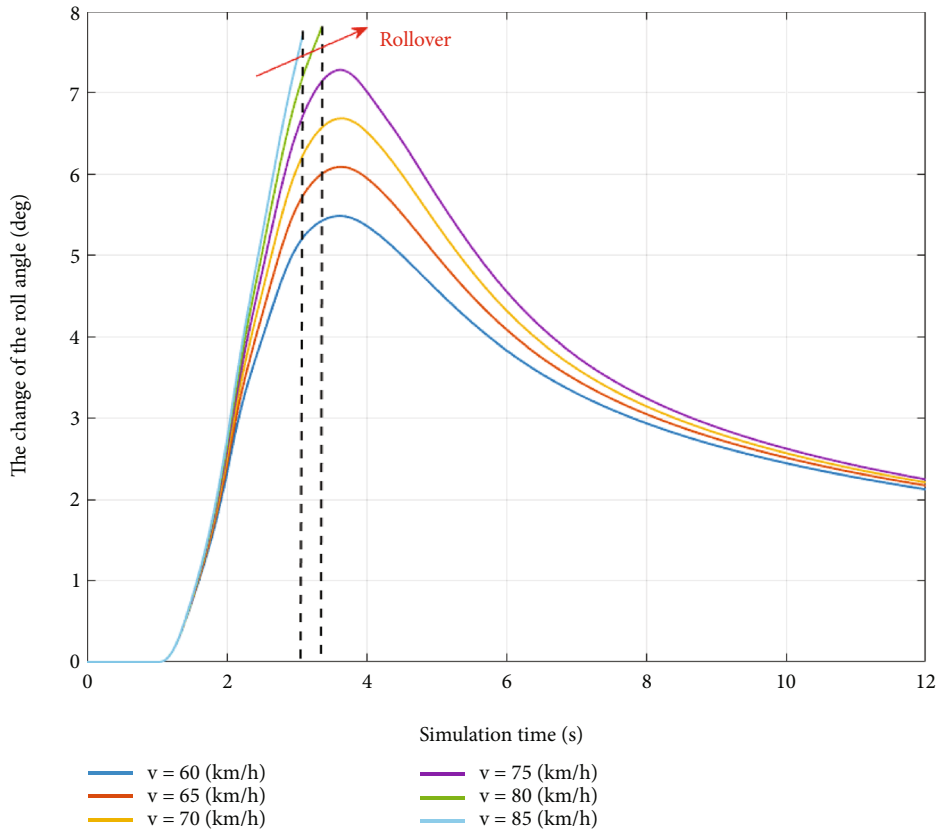

Figure 8: The change of the roll angle (the second case—velocity change).

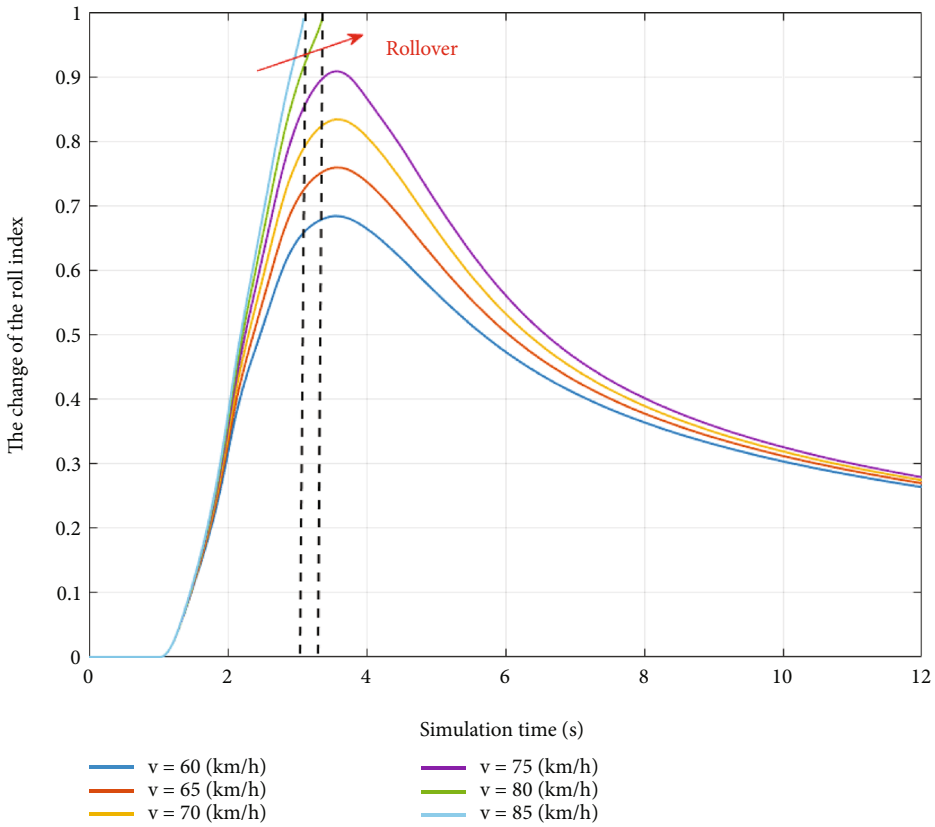

Figure 9: The change of the roll index (the second case—velocity change).

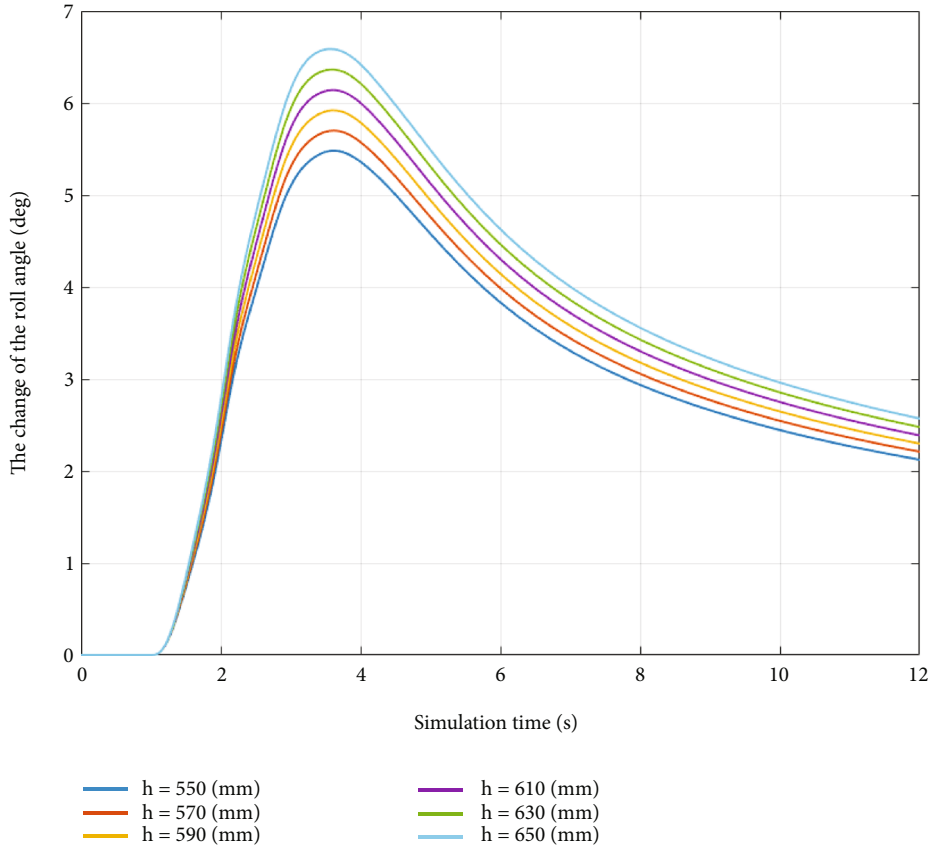

Figure 10: The change of the roll angle (the second case—distance change).

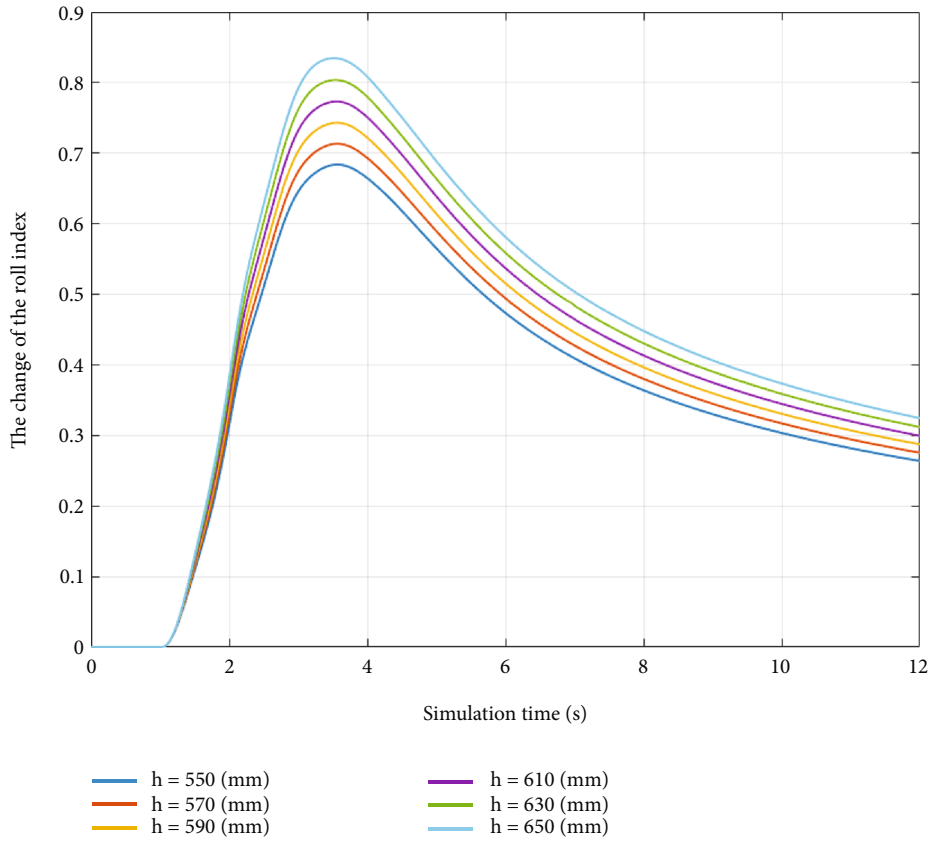

Figure 11: The change of the roll index (the second case—distance change).

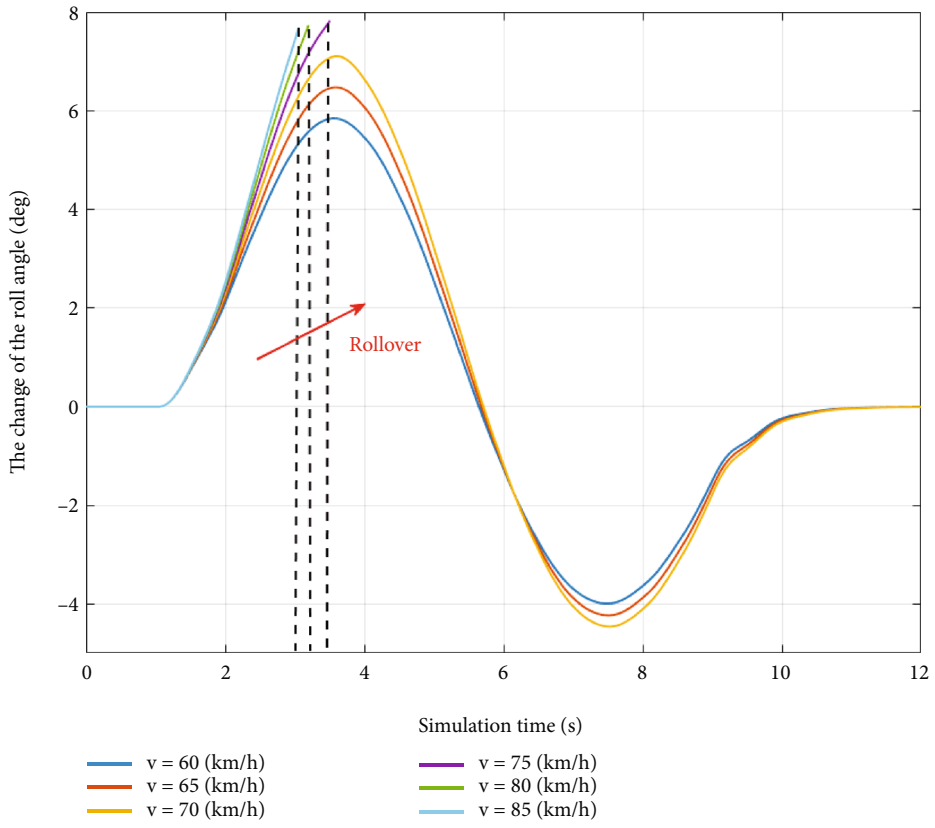

Figure 12: The change of the roll angle (the third case—velocity change).

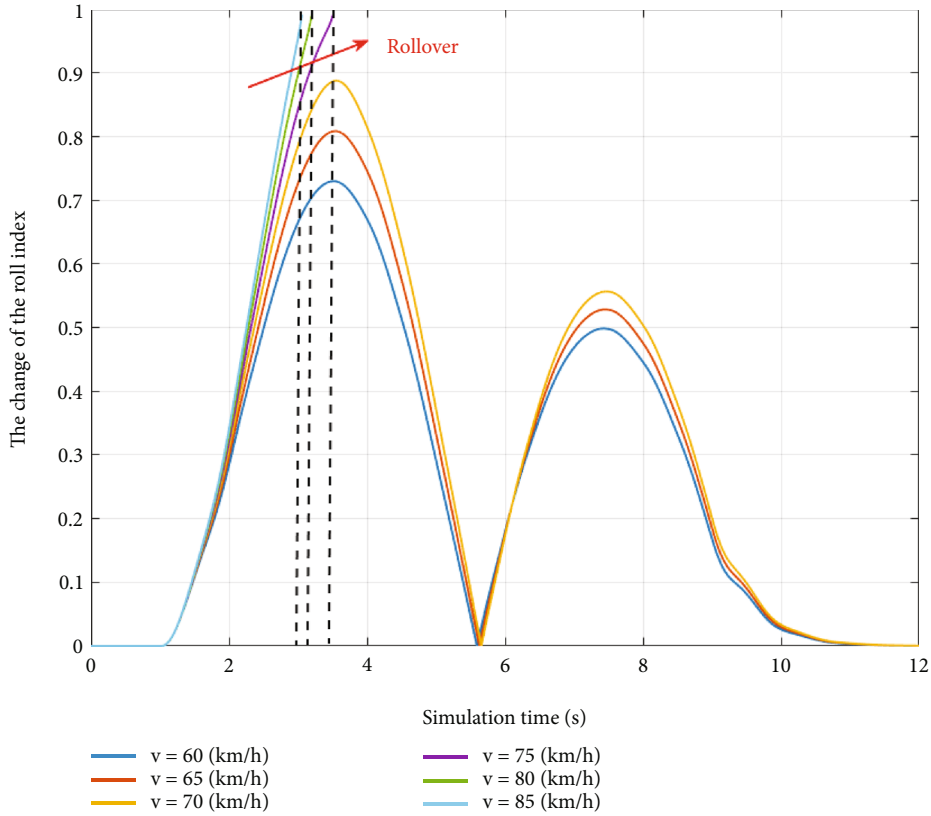

Figure 13: The change of the roll index (the third case—velocity change).

3.2. Second Case. The steering angle in the first case is relatively small, so it is necessary to use a larger steering angle to investigate the car's oscillations comprehensively. In the second case, the values of the steering angle and the steering acceleration increase (Figure 3). The change of the roll angle at a fixed distance, $h = 550$ (mm), and the difference in speed are shown in Figure 8. According to this result, if the velocity rises, the roll angle increases accordingly. The peak values of the roll angle at speeds from 60 to 75 (km/h) are 5.47°, 6.09°, 6.68°, and 7.28°, respectively. At higher speeds, $v = 80$ (km/h), the rollover occurs at time $t \approx 7.8$ (s), i.e., the vertical force at the wheel approaches zero. The main cause of this phenomenon is that the steering angle is too large, and the vehicle is traveling at high speed, which causes the vehicle's roll angle to increase suddenly and drastically reduce the value of the vertical force at the wheel. Once the car is rolled over, the roll angle will reach its maximum value. In this situation, the peak value of the roll angle goes up to 7.77°. Once the speed increases, $v = 85$ (km/h), the car rolls over earlier at time $t \approx 3.1$ (s). So, the maximum roll angle will be smaller, only about 7.63°.

Once a rollover occurs, the value of the roll index approaches 1, as demonstrated in Figure 9. This index can be reduced if the vehicle uses modern anti-roll systems, decreasing the risk of rolling over.

Compared with the above situation, if the speed is fixed at $v = 60$ (km/h) and the distance changes, the rollover may not occur (Figure 10). This is not to say that velocity has a more significant influence than the distance in the car's rollover mechanism. The roll angle variation also highly depends on the range of speeds and distances chosen to perform the simulation. Generally, the changing trend of the roll angle and roll index in the second case is similar to the first. However, their value is larger than in the other case. If the peak of the roll angle is not too large, the value of RI will also not be considerable (Figure 11).

3.3. Third Case. In both cases mentioned above, only the J-turn steering angle is used. Therefore, it is necessary to use another steering angle to describe the vehicle's oscillation. A sine-like steering angle, which describes the double lane change of the vehicle, is shown in the third case. The amplitude of this steering angle is larger than the amplitude of both the first and second cases.

During the first oscillation phase, the roll angle of the vehicle body increases rapidly (Figure 12). Their peak values reach 5.84°, 6.47°, and 7.11°, respectively, with the speed $v = \{60, 65, 70\}$ (km/h). If the speed increases to $v = 75$ (km/h), a rollover will occur. The limited roll angle that the vehicle can achieve is 7.82°. Once the speed reaches $v = 80$ (km/h) or $v = 85$ (km/h), rollover occurs sooner. Therefore, the limited roll angle is only 7.74° and 7.68°, respectively, for these two velocity values. In the second phase of the oscillation, the value of the vehicle body roll angle is smaller than that of the first phase. This is because of the elastic deformation of the tire caused when using a nonlinear tire model. In general, as the speed increases, the roll angle also increases accordingly.

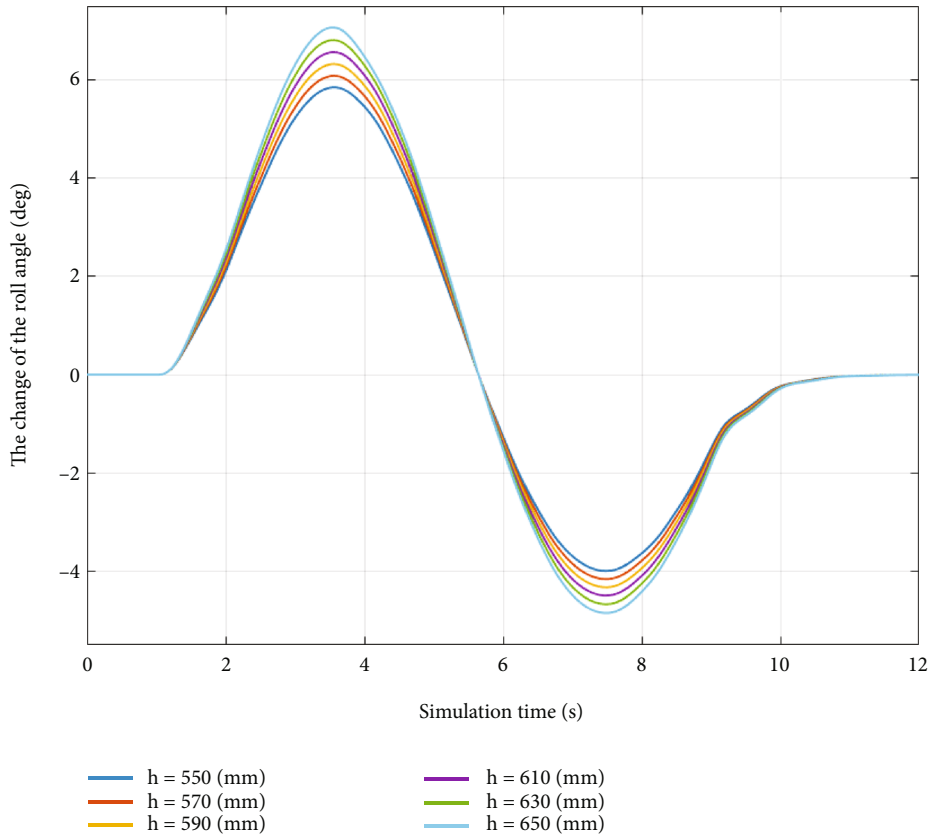

Figure 14: The change of the roll angle (the third case—distance change).

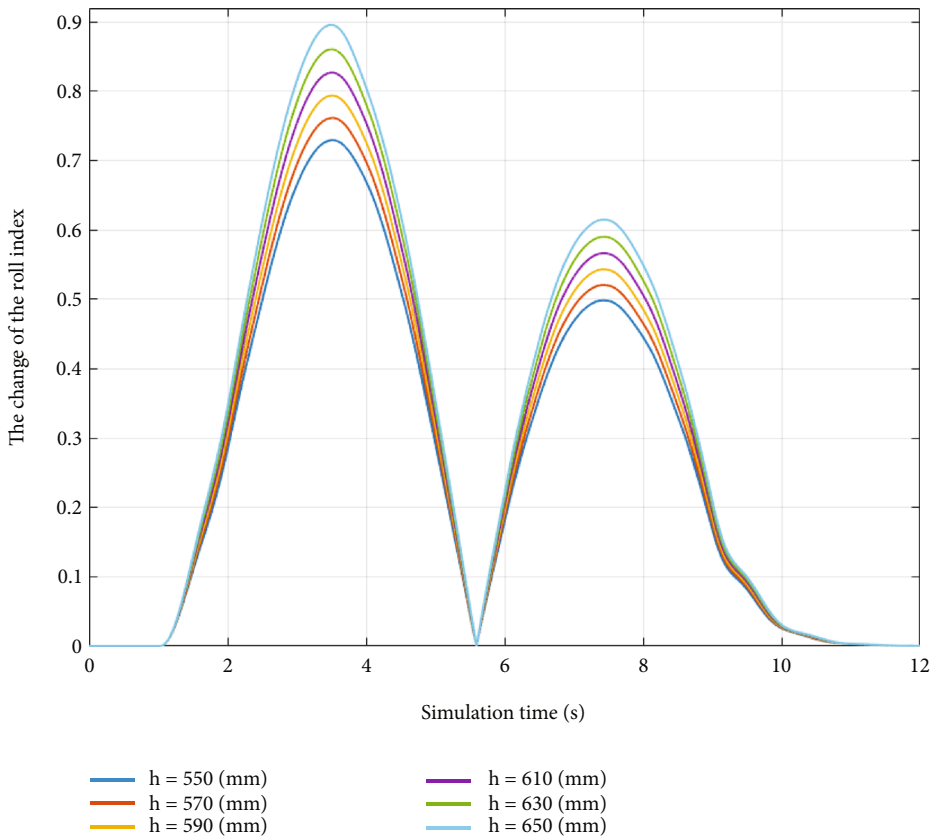

Figure 15: The change of the roll index (the third case—distance change).

The rollover phenomenon is more clearly described by the rollover index (RI) (Figure 13). Their values have approached 1, corresponding to situations where the vehicle has a speed of $v = \{75, 80, 85\}$ (km/h). Meanwhile, the value of RI obtained is smaller as the vehicle's speed decreases.

Figures 14 and 15 depict a situation where the height is changed while the velocity is fixed. According to this finding, the roll angle and rollover index values increase with increasing height. The increase is relatively even. However, the rollover phenomenon does not occur even when the car's moving speed is up to $v = 85$ (km/h). In this situation, the peak value of the roll angle is only 7.06°, corresponding to RI = 0.90. It can be seen that the influence of velocity is more significant than that of distance (this is only true in the situation under consideration).

4. Conclusions

The phenomenon of vehicle rollover usually occurs when the driver makes a sudden turn to avoid obstacles. Therefore, it depends a lot on the steering angle and steering acceleration. Besides, this phenomenon also depends on the speed of travel as well as the size of the vehicle. This phenomenon occurs once the vehicle body's roll angle reaches the limit state, i.e., the vertical force at the wheel is reduced to zero. The consequences of this phenomenon are often very severe, so it is necessary to identify the factors affecting the rollover and prevent it.

In this paper, the author has established a complex dynamic model to simulate vehicle oscillation. This complex model includes component models such as the spatial oscillation model, nonlinear motion model, and nonlinear tire model. The simulation takes place in three specific cases in the MATLAB® environment. In each case, the factors' values are changed flexibly, so that a comprehensive assessment of the dependence of the roll angle on other factors can be made.

According to research findings, the roll angle can increase if the speed or height increases. Besides, if the steering angle is more significant, this angle will also be larger. This results in an increased rollover index and a higher risk of a rollover. Therefore, the driver should not suddenly steer at high speed to prevent the vehicle from rolling over. Besides, the height of the vehicle body should be limited, and the trackwidth should also be extended. The results of this study are entirely novel and unique. These results will be the database for other studies in the future.

Abbreviations

ϕ: Roll angle, rad
θ: Pitch angle, rad
ψ: Yaw angle, rad
δ_{ij}: Steering angle, rad
a_1: Distance from the center to front axle, m
a_2: Distance from the center to rear axle, m
F_1/F_2: External force, N
F_{cex}: Centrifugal force (longitudinal), N
F_{cey}: Centrifugal force (lateral), N
F_{Cij}: Damper force, N
F_{ims}: Sprung mass forces, N
F_{imuij}: Sprung mass forces, N
F_{ix}: Inertia force (longitudinal), N
F_{iy}: Inertia force (lateral), N
F_{Kij}: Spring force, N
F_{KTij}: Tire force, N
F_{xij}: Tire force (longitudinal), N
F_{yij}: Tire force (lateral), N
g: Gravitational acceleration, m/s^2
h_ϕ: Distance from the center to roll axis, m
M_ϕ: Sprung mass moments (roll), Nm
M_θ: Sprung mass moments (pitch), Nm
M_ψ: Total moments (yaw), Nm
t_{wi}: Half of the track width, m
v_x: Vehicle velocity (longitudinal)
v_y: Vehicle velocity (lateral)
z_s: Vertical sprung mass displacement, m
z_{uij}: Vertical unsprung mass displacement, m
β: Heading angle, rad.

Data Availability

The data used to support the findings of this study are included within the article.

Conflicts of Interest

The authors declare that there is no conflict of interest regarding the publication of this paper.

Acknowledgments

This research received no specific grant from any funding agency in the public, commercial, or not-for-profit sectors.

References

[1] A. J. Anarkooli, M. Hosseinpour, and A. Kardar, "Investigation of factors affecting the injury severity of single-vehicle rollover crashes: a random-effects generalized ordered probit model," *Accident Analysis and Prevention*, vol. 106, pp. 399–410, 2017.

[2] A. H. Kazemian, M. F. Mahani, and H. Darijani, "Rollover index for the diagnosis of tripped and untripped rollovers," *Latin American Journal of Solids and Structures*, vol. 14, no. 11, pp. 1979–1999, 2017.

[3] T. A. Nguyen, "Preventing the rollover phenomenon of the vehicle by using the hydraulic stabilizer bar controlled by a two-input fuzzy controller," *IEEE Access*, vol. 9, pp. 129168–129177, 2021.

[4] T. A. Nguyen, "Improving the stability of the passenger vehicle by using an active stabilizer bar controlled by the fuzzy method," *Complexity*, vol. 2021, p. 20, 2021.

[5] T. A. Nguyen, "Determination of the rollover limitation of a vehicle when moving by 4-dimensional plots," *Advances in Systems Science and Applications*, vol. 22, no. 3, pp. 96–105, 2022.

[6] M. Seyedi, S. Jung, J. Wekezer, J. R. Kerrigan, and B. Gepner, "Rollover crashworthiness analyses—an overview and state of

the art," *International Journal of Crashworthiness*, vol. 25, no. 3, pp. 328–350, 2020.

[7] A. N. Tuan and B. H. Thang, "Research on dynamic vehicle model equipped active stabilizer bar," *Advances in Science, Technology and Engineering Systems Journal*, vol. 4, no. 4, pp. 271–275, 2019.

[8] Q. Zhang, C. Su, Y. Zhou, C. Zhang, J. Ding, and Y. Wang, "Numerical investigation on handling stability of a heavy tractor semi-trailer under crosswind," *Applied Sciences*, vol. 10, no. 11, p. 3672, 2020.

[9] N. Ikhsan, A. Saifizul, and R. Ramli, "The effect of vehicle and road conditions on rollover of commercial heavy vehicles during cornering: a simulation approach," *Sustainability*, vol. 13, no. 11, p. 6337, 2021.

[10] D. N. Nguyen, T. A. Nguyen, T. B. Hoang, and N. D. Dang, "Establishing the method to predict the limited roll angle of the vehicle based on the basic dimensions," *Mathematical Modelling of Engineering Problems*, vol. 8, no. 5, pp. 775–779, 2021.

[11] B. Li and S. Bei, "Research method of vehicle rollover mechanism under critical instability condition," *Advances in Mechanical Engineering*, vol. 11, no. 1, 2019.

[12] T. Xin, J. Xu, C. Gao, and Z. Sun, "Research on the speed thresholds of trucks in a sharp turn based on dynamic rollover risk levels," *PLoS One*, vol. 16, no. 8, p. e0256301, 2021.

[13] D. Shin, S. Woo, and M. Park, "Rollover Index for Rollover Mitigation Function of Intelligent Commercial Vehicle's Electronic Stability Control," *Electronics*, vol. 10, no. 21, p. 2605, 2021.

[14] Z. Jin, J. Li, Y. Huang, and A. Khajepour, "Study on rollover index and stability for a triaxle bus," *Chinese Journal of Mechanical Engineering*, vol. 32, no. 1, p. 15, 2019.

[15] M. Ataei, A. Khajepour, and S. Jeon, "A general rollover index for tripped and un-tripped rollovers on flat and sloped roads," *Proceedings of the Institution of Mechanical Engineers, Part D: Journal of Automobile Engineering*, vol. 233, no. 2, pp. 304–316, 2019.

[16] X. Zhang, Y. Yang, K. Guo, J. Lv, T. Peng et al., "Contour line of load transfer ratio for vehicle rollover prediction," *Vehicle System Dynamics*, vol. 55, no. 11, pp. 1748–1763, 2017.

[17] S. Zhang, S. Bei, B. Li, Y. Jin, and H. Yan, "Overview of car rollover system development," *Advances in Engineering Research*, vol. 154, pp. 275–282, 2018.

[18] A. Chokor, R. Talj, and A. Charara, "Effect of roll motion control on vehicle lateral stability and rollover avoidance," *American Control Conference*, pp. 4868–4875, 2020.

[19] L. Zhao and Z. Liu, "Vehicle velocity and roll angle estimation with road and friction adaptation for four-wheel independent drive electric vehicle," *Mathematical Problems in Engineering*, vol. 2014, p. 11, 2014.

[20] X. Li, J. Li, L. Su, and Y. Cao, "Study on roll instability mechanism and stability index of articulated steering vehicles," *Mathematical Problems in Engineering*, vol. 2016, p. 14, 2016.

[21] T. A. Nguyen, "Control the hydraulic stabilizer bar to improve the stability of the vehicle when steering," *Mathematical Modelling of Engineering Problems*, vol. 8, no. 2, pp. 199–206, 2021.

[22] T. A. Nguyen, "New methods for calculating the impact force of the mechanical stabilizer bar on a vehicle," *International Journal on Engineering Applications*, vol. 9, no. 5, pp. 251–257, 2021.

[23] H. Qi, N. Zhang, Y. Chen, and B. Tan, "A comprehensive tune of coupled roll and lateral dynamics and parameter sensitivity study for a vehicle fitted with hydraulically interconnected suspension system," *Proceedings of the Institution of Mechanical Engineers, Part D: Journal of Automobile Engineering*, vol. 235, no. 1, pp. 143–161, 2020.

[24] D. N. Nguyen, T. A. Nguyen, and N. D. Dang, "A novel sliding mode control algorithm for an active suspension system considering with the hydraulic actuator," *Latin American Journal of Solids and Structures*, vol. 19, no. 1, 2022.

[25] T. A. Nguyen, "Advance the efficiency of an active suspension system by the sliding mode control algorithm with five state variables," *IEEE Access*, vol. 9, pp. 164368–164378, 2021.

[26] J. Konieczny, M. Sibielak, and W. Raczka, "Active vehicle suspension with anti-roll system based on advanced sliding mode controller," *Energies*, vol. 13, no. 21, p. 5560, 2020.

[27] M. Dong, Y. Fan, D. Yu, Q. Wang et al., "Research on electric vehicle rollover prevention system based on motor speed control," *World Electric Vehicle Journal*, vol. 12, no. 4, p. 195, 2021.

[28] L. P. González, S. S. Sánchez, J. Garcia-Guzman, M. J. L. Boada, and B. L. Boada, "Simultaneous estimation of vehicle roll and sideslip angles through a deep learning approach," *Sensors*, vol. 20, no. 13, p. 3679, 2020.

[29] J. G. Guzmán, L. P. González, J. P. Redondo, M. M. M. Martínez, and M. J. L. Boada, "Real-time vehicle roll angle estimation based on neural networks in IoT low-cost devices," *Sensors*, vol. 18, no. 7, 2018.

[30] J. G. Guzmán, L. P. Gonzalez, J. P. Redondo, S. S. Sanchez, and B. L. Boada, "Design of low-cost vehicle roll angle estimator based on Kalman filters and an IoT architecture," *Sensors*, vol. 18, no. 6, p. 1800, 2018.

[31] R. Bencatel, R. Tian, A. R. Girard, and I. Kolmanovsky, "Reference governor strategies for vehicle rollover avoidance," *IEEE Transactions on Control Systems Technology*, vol. 26, no. 6, pp. 1954–1969, 2018.

[32] B. Edlund, O. Lindroos, and T. Nordfjell, "The effect of rollover protection systems and trailers on quad bike stability," *International Journal of Forest Engineering*, vol. 31, no. 2, pp. 95–105, 2020.

[33] Y. Liu, K. Yang, X. He, and X. Ji, "Active Steering and Anti-Roll Shared Control for Enhancing Roll Stability in Path Following of Autonomous Heavy Vehicle," *SAE Technical Paper*, 2019.

[34] D. N. Nguyen, T. A. Nguyen, and N. D. Dang, "A complex rollover dynamics model with active stabilizer bar controlled by the fuzzy algorithm," *Heliyon*, vol. 8, no. 11, p. e11715, 2022.

[35] H. Sun, Y. H. Chen, and H. Zhao, "Adaptive robust control methodology for active roll control system with uncertainty," *Nonlinear Dynamics*, vol. 92, no. 2, pp. 359–371, 2018.

[36] A. Tota, L. Dimauro, F. Velardocchia, G. Paciullo, and M. Velardocchia, "An intelligent predictive algorithm for the anti-rollover prevention of heavy vehicles for off-road applications," *Machines*, vol. 10, no. 10, p. 835, 2022.

[37] A. Alrejjal, A. Farid, and K. Ksaibati, "Investigating factors influencing rollover crash risk on mountainous interstates," *Journal of Safety Research*, vol. 80, pp. 391–398, 2022.

[38] M. A. Hassan, M. A. A. Abdelkareem, M. M. Moheyeldein, A. Elagouz, and G. Tan, "Advanced study of tire characteristics and their influence on vehicle lateral stability and untripped rollover threshold," *Alexandria Engineering Journal*, vol. 59, no. 3, pp. 1613–1628, 2020.

[39] A. Alrejjal and K. Ksaibati, "Impact of crosswinds and truck weight on rollover propensity when negotiating combined curves," *International Journal of Transportation Science and Technology*, 2022.

[40] H. Wang, B. Liu, X. Ping, and Q. An, "Path tracking control for autonomous vehicles based on an improved MPC," *IEEE Access*, vol. 7, pp. 161064–161073, 2019.

[41] D. Lee, S. Jin, and C. Lee, "Deep reinforcement learning of semi-active suspension controller for vehicle ride comfort," *IEEE Transactions on Vehicular Technology*, vol. 72, no. 1, pp. 327–339, 2023.

[42] H. Wang, W. Cui, Z. Xia, and W. Jiang, "Vehicle lane keeping system based on TSK fuzzy extension control," *Proceedings of the Institution of Mechanical Engineers, Part D: Journal of Automobile Engineering*, vol. 234, no. 2–3, pp. 762–773, 2020.